



Universiteit
Leiden
The Netherlands

A DROP-IN gamma probe for robot-assisted radioguided surgery of lymph nodes during radical prostatectomy

Dell'Oglio, P.; Meershoek, P.; Maurer, T.; Wit, E.M.K.; Leeuwen, P.J. van; Poel, H.G. van der; ... ; Oosterom, M.N. van

Citation

Dell'Oglio, P., Meershoek, P., Maurer, T., Wit, E. M. K., Leeuwen, P. J. van, Poel, H. G. van der, ... Oosterom, M. N. van. (2021). A DROP-IN gamma probe for robot-assisted radioguided surgery of lymph nodes during radical prostatectomy. *European Urology*, 79(1), 124-132. doi:10.1016/j.eururo.2020.10.031

Version: Publisher's Version

License: [Creative Commons CC BY 4.0 license](https://creativecommons.org/licenses/by/4.0/)

Downloaded from: <https://hdl.handle.net/1887/3277320>

Note: To cite this publication please use the final published version (if applicable).

available at www.sciencedirect.com
journal homepage: www.europeanurology.com



Surgery in Motion

A DROP-IN Gamma Probe for Robot-assisted Radioguided Surgery of Lymph Nodes During Radical Prostatectomy

Paolo Dell'Oglio^{a,b,c,d}, Philippa Meershoek^{a,c}, Tobias Maurer^e, Esther M.K. Wit^c,
Pim J. van Leeuwen^c, Henk G. van der Poel^c, Fijs W.B. van Leeuwen^{a,b,c},
Matthias N. van Oosterom^{a,c,*}

^a Interventional Molecular Imaging Laboratory, Department of Radiology, Leiden University Medical Center, Leiden, The Netherlands; ^b ORSI Academy, Melle, Belgium; ^c Department of Urology, Netherlands Cancer Institute-Antoni van Leeuwenhoek Hospital, Amsterdam, The Netherlands; ^d Department of Urology, ASST Grande Ospedale Metropolitano Niguarda, Milan, Italy; ^e Martini-Clinic, University Medical Center Hamburg-Eppendorf, Hamburg, Germany

Article info

Article history:

Accepted October 22, 2020

Associate Editor:

Alexandre Mottrie

Keywords:

Fluorescence imaging
Gamma probe
Image-guided surgery
Prostate cancer
Radioguided surgery
Robotic surgery
Sentinel lymph node

Please visit

www.europeanurology.com and
www.urosources.com to view the
accompanying video.

Abstract

Background: The DROP-IN gamma probe was introduced to overcome the restricted manoeuvrability of traditional laparoscopic gamma probes. Through enhanced manoeuvrability and surgical autonomy, the DROP-IN promotes the implementation of radioguided surgery in the robotic setting.

Objective: To confirm the utility and safety profile of the DROP-IN gamma probe and to perform a comparison with the traditional laparoscopic gamma probe and fluorescence guidance.

Design, setting, and participants: Twenty-five prostate cancer patients were scheduled for a robot-assisted sentinel lymph node (SN) procedure, extended pelvic lymph node dissection, and prostatectomy at a single European centre.

Surgical procedure: After intraprostatic injection of indocyanine green (ICG)-^{99m}Tc-nanocolloid ($n = 12$) or ^{99m}Tc-nanocolloid + ICG ($n = 13$), SN locations were defined using preoperative imaging. Surgical excision of SNs was performed under image guidance using the DROP-IN gamma probe, the traditional laparoscopic gamma probe, and fluorescence imaging.

Measurements: Intraoperative SN detection was assessed for the different modalities and related to anatomical locations. Patient follow-up was included (a median of 18 mo).

Results and limitations: Overall, 47 SNs were pursued in vivo by the DROP-IN gamma probe, of which 100% were identified. No adverse events related to its use were observed. In vivo fluorescence imaging identified 91% of these SNs. The laparoscopic gamma probe identified only 76% of these SNs, where the detection inaccuracies appeared to be related to specific anatomical regions.

Conclusions: Owing to improved manoeuvrability, the DROP-IN probe yielded improved SN detection rates compared with the traditional gamma probe and fluorescence imaging. These findings underline that the DROP-IN technology provides a valuable tool for radioguided surgery in the robotic setting.

Patient summary: Radioguided robot-assisted surgery with the novel DROP-IN gamma probe is feasible and safe. It enables more efficient intraoperative identification of sentinel lymph nodes than can be achieved with a traditional laparoscopic gamma probe. The use of the DROP-IN probe in combination with fluorescence imaging allows for a complementary optical confirmation of node localisations.

© 2020 The Author(s). Published by Elsevier B.V. on behalf of European Association of Urology. This is an open access article under the CC BY license (<http://creativecommons.org/licenses/by/4.0/>).

* Corresponding author. Interventional Molecular Imaging Laboratory, Department of Radiology, Leiden University Medical Center, Albinusdreef 2, 2300 RC Leiden, The Netherlands.

Tel. +31-(0)715262042.

E-mail address: m.n.van_oosterom@lumc.nl (M.N. van Oosterom).



1. Introduction

Extended pelvic lymph node dissection (ePLND) in prostate cancer (PCa) is curative for a small subset of patients with limited lymph node (LN) involvement (direct effect of ePLND) [1,2]. The procedure also allows for the identification of patients who have survival benefit from adjuvant treatments (indirect effect of ePLND) [3]. This makes ePLND the best available staging tool for PCa patients with a risk of LN invasion of >5%, as suggested by the European Association of Urology [4]. Unfortunately, excision of the ePLND template misses up to 35% of the potential landing sites for lymph nodal metastases [5–9]. Personalised lymphatic mapping procedures such as sentinel node (SN) biopsy help extend the ePLND template in a personalised manner [10]. Wit et al [11] underscore that such an extension creates a clinical impact, where combined usage of SN and ePLND showed that 73% of the metastatic nodes were SNs, and in one out of 20 patients, metastatic nodes are missed without the SN procedure.

Similar to many surgical technologies, radioguidance found its birth during open surgery [12], a setting where a traditional gamma probe can be positioned with optimal rotational freedom [11]. Unfortunately, application of such rigid gamma probes during laparoscopic surgery has several drawbacks. Namely, the rotation point defined by the trocars restricts the rotational freedom and thus the ability to reach certain anatomical locations [13]. Robot-assisted

laparoscopic surgery further complicates this, as the surgeon is no longer present at the bedside to handle the laparoscopic gamma probe. Recently, a robotic-tailored radioguidance modality (ie, the DROP-IN gamma probe; Fig. 1) was developed to (1) increase the rotational freedom in probe positioning, (2) limit interference in the surgical workflow, and (3) allow autonomous probe positioning via the robotic console [13,14].

In the field of surgical guidance, the use of radioactivity is increasingly receiving competition from nonradioactive alternatives (eg, fluorescence or magnetism based) [10]. One motivation for the widespread robot use of fluorescence is the integration of Firefly fluorescence laparoscopes in the recent da Vinci robotic platforms, combined with the above-mentioned limitation of laparoscopic gamma probes [15,16]. Studies that explore the combined use of radioguidance and fluorescence guidance in robot-assisted urological surgery indicate that fluorescence imaging can be used to refine single-photon emission computed tomography (SPECT)/computed tomography (CT) and gamma-probe based radioguidance procedures, but has poor detection sensitivity when used alone [17,18].

The aim of the current study was to further extend the patient cohort as published in our first-in-human feasibility study [14], investigate follow-up, confirm the technical advantage and safety profile of the DROP-IN gamma probe technology during SN + ePLND + robot-assisted radical prostatectomy (RARP), and illustrate the surgical technique



Fig. 1 – Zoomed-in photograph of the prototype DROP-IN gamma probe as grasped by a ProGrasp instrument of the da Vinci surgical robot. Copyright H.J.F. van de Stadt (used with permission).

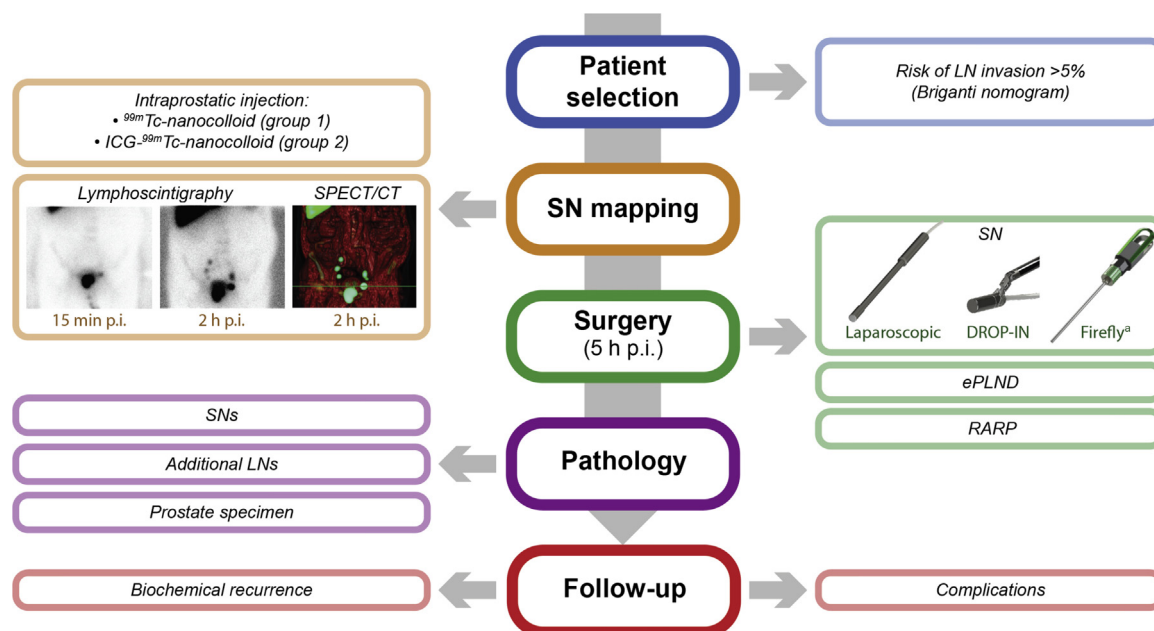


Fig. 2 – Flowchart of the study design, describing the steps taken from patient selection to follow-up. CT = computed tomography; ePLND = extended pelvic lymph node dissection; ICG = indocyanine green; LN = lymph node; p.i. = post injection; RARP = robot-assisted radical prostatectomy; SN = sentinel node; SPECT = single-photon emission computed tomography. ^aTo allow for fluorescence imaging in group 1, an additional intraprostatic injection with ICG was given in the operating room, at the start of surgery.

(accompanying video). In doing so, we provided the first quantitative comparison of the DROP-IN gamma probe, the traditional rigid laparoscopic gamma probe, and Firefly fluorescence imaging.

2. Patients and methods

2.1. Surgical hardware

Robot-assisted surgical procedures were performed with a da Vinci Si system (Intuitive Surgical Inc., USA). Radioguidance was provided with a prototype DROP-IN gamma probe (Eurorad S.A., France; sterilised using a STERRAD 100S sterilisation protocol; Fig. 1) and a Europrobe laparoscopic 0° gamma probe (Eurorad S.A.; used with a sterile cover). Both the laparoscopic and the DROP-IN probe provide an acoustic and numeric feedback as to the presence of radiotracers within the tissue evaluated and make use of the same type of read-out module. Fluorescence guidance was provided by the robot-integrated Firefly laparoscope (in vivo) and an open surgery fluorescence camera (FIS-00; Hamamatsu Photonics K.K., Japan; ex vivo).

2.2. Patient population and preoperative SN mapping

The clinical evaluation relied on 25 PCa patients scheduled for a robot-assisted SN procedure, ePLND, and RARP between December 2017 and December 2018, performed by three experienced surgeons. All these patients had a preoperative risk of LN invasion of >5% (nomogram by Briganti et al [19]; Fig. 2).

Preoperative SN mapping was performed with early and late dynamic lymphoscintigraphy, respectively, 15 min and 2 h after injection. This was followed by SPECT supplemented with low-dose CT (2 h after injection; Fig. 3A). Patients were randomly assigned to receive an SN tracer injection with either ^{99m}Tc -nanocolloid (group 1;

$n = 13$, 52%) or the hybrid tracer ICG- ^{99m}Tc -nanocolloid (group 2; $n = 12$, 48%). Both tracers were transrectally injected into the peripheral zone of each quadrant of the prostate, under ultrasound guidance, as described previously [15]. The nuclear medicine physician assessed all images to determine the number and location of the SNs. Surgery was planned about 5 h after tracer injection. To allow for fluorescence imaging, patient group 1 received an additional intraprostatic injection of ICG at the start of surgery. This study was approved by the local ethical committee (study number NL57838.031.16), and all patients provided informed consent.

2.3. Surgical procedure

All procedures were performed through a six-port transperitoneal approach using the four-arm da Vinci robot. Preoperative SPECT/CT served as a roadmap of the number and location of SNs with respect to the anatomical context [15]. Suspected SN locations were scanned in vivo with the DROP-IN and traditional laparoscopic gamma probes. The DROP-IN probe could be used either through the 12 mm assistant trocar placed within the Alexis laparoscopic system (Applied Medical Corp., USA; placed 4 cm cranial to the iliac crest on the right side of the patient) or next to this trocar (Fig. 4B). Conversely, the traditional laparoscopic gamma probe was used only through the 12 mm trocar, blocking its further use completely. The DROP-IN probe, on the contrary, still allowed space for smaller instruments (ie, suction/respiration; Fig. 4B). Hence, the DROP-IN could remain at the surgeon's disposal, while the laparoscopic probe had to be inserted and retracted, by the bedside assistant, upon the surgeon's command. The DROP-IN probe was autonomously grasped and manoeuvred by the surgeon using the surgical console and the da Vinci ProGrasp Forceps. Firefly imaging was used to achieve fluorescence guidance.

The intraoperatively detected SN locations were directly verified with preoperative SPECT/CT mapping. When the operating surgeon decided that the SN was located in anatomical regions where resection

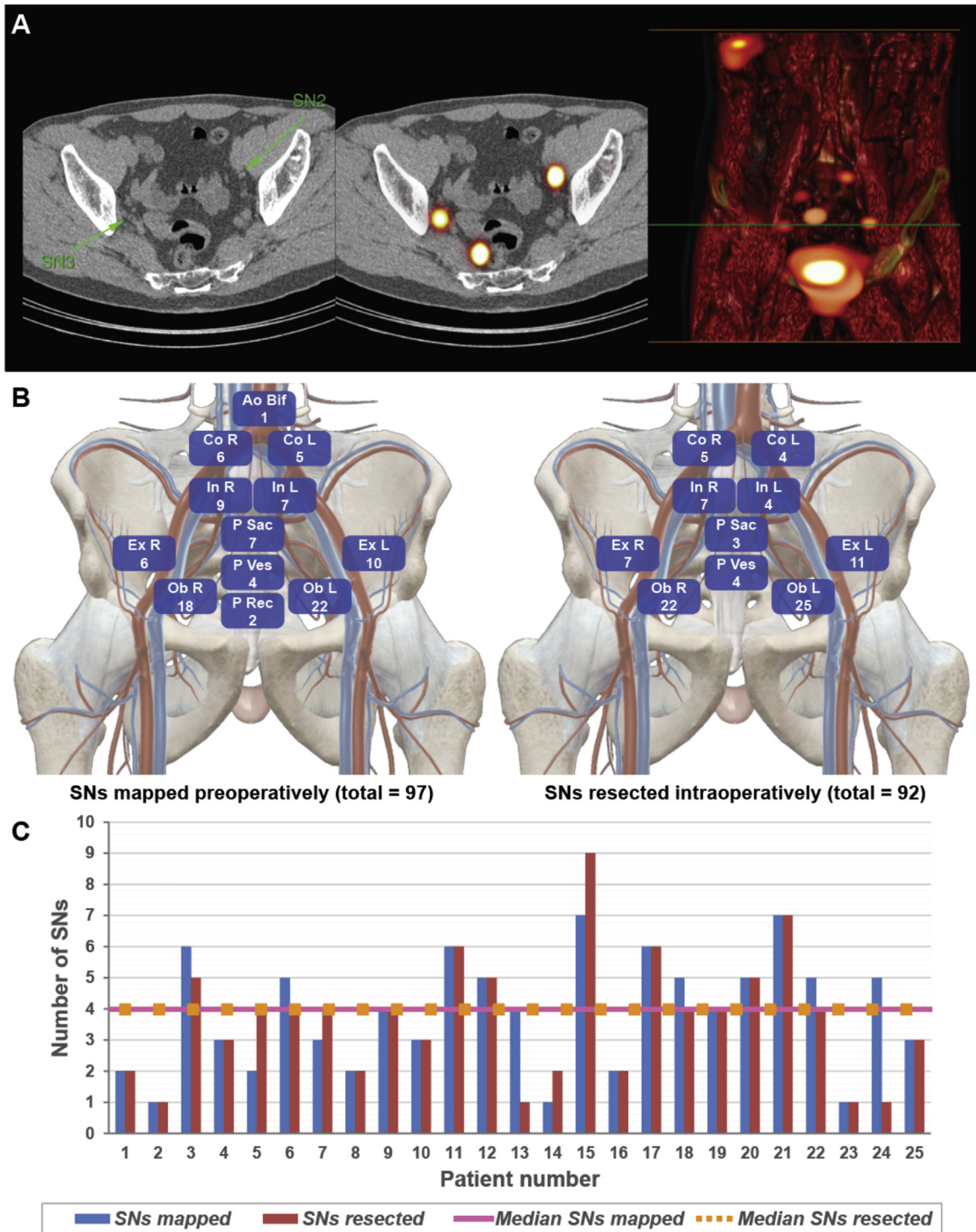


Fig. 3 – Preoperative mapping and intraoperative resection of the SNs: (A) SN mapping after either ^{99m}Tc-nanocolloid or ICG-^{99m}Tc-nanocolloid intraprostatic injection using single-photon emission computed tomography supplemented with computed tomography (SPECT/CT); SNs (B) mapped preoperatively and (C) resected intraoperatively according to anatomical location; (D) median of SNs mapped preoperatively and resected intraoperatively. Ao Bif= aortic bifurcation; Co = common; Ex = external; ICG = indocyanine green; In = internal; L = left; Ob = obturator; P rec = pararectal; P sac = presacral; P ves = paravesical; R = right; SN = sentinel node.

would potentially yield a high risk of surgical complications (eg, presacral, pararectal, or high along the aorta [20]), it was left in situ. After excision of the SNs, the surgical bed was carefully re-examined. Once removed, all SNs underwent ex vivo radioactive (DROP-IN and laparoscopic probe) and fluorescence examination (FIS-00).

The ePLND template was defined as the region encompassed by the ureteric crossing and including the bifurcation of the common iliac artery, along the external iliac (the distal limit being the deep circumflex vein and femoral canal), the internal iliac vessels, and the obturator fossa. The lateral border was the genitofemoral nerve and the medial border

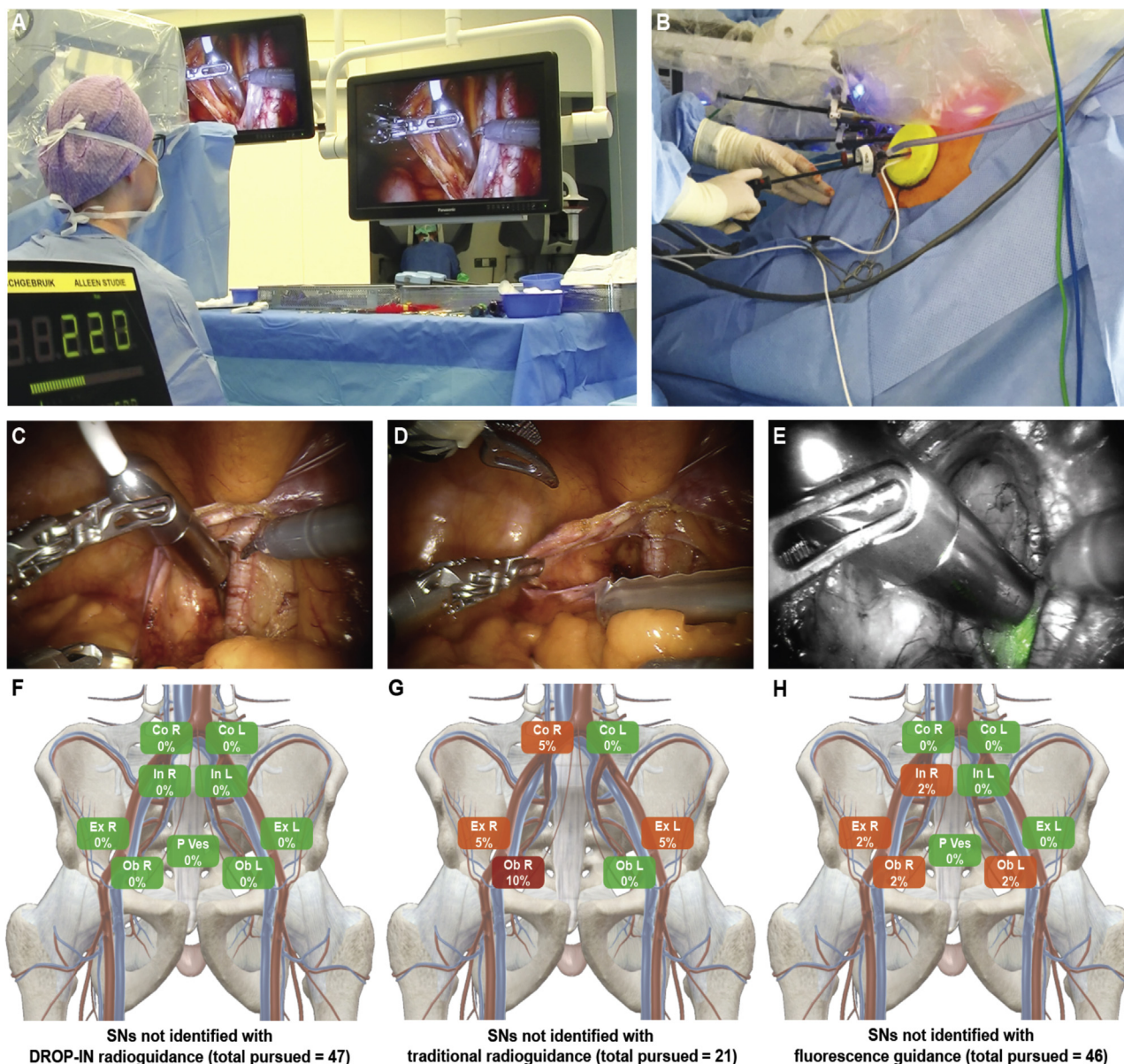


Fig. 4 – In vivo guidance of the DROP-IN probe versus laparoscopic gamma probe versus Firefly fluorescence laparoscope: (A) overview of the operating room layout using the DROP-IN gamma probe in robotic surgery, showing the probe console with audible and numerical feedback in the lower left corner of the image. (B) The DROP-IN probe is inserted next to the 12 mm assistant trocar placed within the Alexis system; in vivo guidance with the (C) DROP-IN probe versus (D) laparoscopic gamma probe versus (E) Firefly fluorescence laparoscope; SN detection with the (F) DROP-IN probe versus (G) laparoscopic gamma probe versus (H) Firefly fluorescence laparoscope, according to anatomical location. Co = common; Ex = external; In = internal; L = left; Ob = obturator; P ves = paravesical; R = right; SN = sentinel node.

the perivesical fat. The SN procedure was always combined with an ePLND and followed by RARP. To minimise the impact on the procedure, in some cases, SNs that occurred within ePLND-template specimens were not pursued with radioguidance or fluorescence guidance in vivo.

2.4. Covariates

All patients included in this study had complete preoperative data including age at surgery, body mass index (BMI), prostate-specific antigen (PSA) at diagnosis, clinical T stage, N stage, biopsy Gleason score, and SNs identified. Pathological data consisted of pathological T stage, N stage, Gleason score, positive surgical margins, SNs removed, LNs

removed, and tumour-positive nodes. Postoperative complications were categorised according to the Clavien-Dindo classification.

Patients underwent follow-up visits every 3 mo during the 1st year and every 6 mo thereafter. Biochemical recurrence (BCR) was defined as two consecutive PSA values of ≥ 0.2 ng/ml [4]. All men with BCR underwent prostate-specific membrane antigen positron emission tomography (PSMA-PET).

2.5. Statistical analysis

Statistical analyses, reporting, and interpretation of the results were conducted according to established guidelines [21]. Medians and

interquartile ranges (IQRs), as well as frequencies and proportions were reported for continuous and categorical variables, respectively. Frequencies and proportions were also used to assess in vivo and ex vivo SN identification according to the DROP-IN probe versus the laparoscopic probe versus fluorescence camera, stratified according to the anatomical location. For all statistical analyses, SPSS statistics (IMB Corp., USA) and Excel (Microsoft Corp., USA) were used.

3. Results

3.1. Preoperative imaging

Patient characteristics are provided in [Table 1](#) and Supplementary Table 1. The median radioactive dose injected in all patients was 205.6 MBq. SNs were identified in all the 25 patients, and no adverse reactions were observed. A total of 97 SNs were identified by preoperative imaging (median four SNs per patient, IQR: 2–5; [Fig. 3A, 3B, and 3D](#)). Of these SNs, 26% were located outside the ePLND template.

3.2. Intraoperative SN identification

The median time from tracer injection to surgery was 5.4 h. A total of 92 SNs were excised (median four SNs per patient, IQR: 2–5; [Fig. 3C and 3D](#)), of which 17% were located outside the ePLND template. Overall, 47 SNs were pursued by the DROP-IN gamma probe (100% could be identified clearly, of which 13% was located outside the ePLND template; [Table 2](#) and [Fig. 4](#)). Of those SNs examined by the DROP-IN probe, 45% (21 SNs; 14 patients) and 98% (46 SNs; 25 patients) were also pursued with the laparoscopic gamma probe and fluorescence, respectively. When the surgeon expected the laparoscopic gamma probe to have little value, its use was omitted. The laparoscopic gamma probe and Firefly fluorescence camera allowed clear identification of, respectively, 76.2% (16/21) and 91.3% (42/46) of the SNs examined ([Table 2](#)). In the case of gamma tracing, the DROP-IN probe showed superiority over the laparoscopic gamma probe for SNs located in the obturator right, external right, common iliac right, and external left regions ([Table 2](#) and [Fig. 4](#)). The traditional laparoscopic gamma probe appeared to be especially restricted in manoeuvrability on the right side of the patient, where the point of entry into the patient (ie, the assistant trocar) was located, as was also confirmed with supplementary phantom experiments (see the Supplementary material). This did not limit the DROP-IN gamma probe, being tethered and containing two extra degrees of freedom. Compared with fluorescence guidance, the DROP-IN probe favoured the detection of SNs located in the obturator left and right, external right, and internal right regions ([Table 2](#) and [Fig. 4](#)). Here, fluorescence detection appeared to be restricted in sensitivity.

Ex vivo examinations with the laparoscopic gamma probe (100% detection) and fluorescence imaging (96% detection) confirmed the individual guidance modalities performed as they were supposed to ([Table 2](#)).

Table 1 – Patient characteristics

Variables	Overall cohort (n = 25)
<i>Preoperative data</i>	
Age (yr), median (IQR)	69 (65–71)
BMI (kg/m ²), median (IQR)	28.5 (28.3–28.7)
PSA (ng/ml), median (IQR)	17 (10.3–24.5)
Clinical T stage, n (%)	
T1	2 (8)
T2	16 (64)
T3	7 (28)
Clinical N stage, n (%)	
N0	25 (100)
ISUP grade group at biopsy, n (%)	
1	1 (4)
2	8 (32)
3	6 (24)
4	6 (24)
5	4 (16)
SNs identified at preoperative imaging, n (median, IQR)	97 (4, 2–5)
<i>Pathological data and follow-up</i>	
Pathological T stage, n (%)	
T2	12 (48)
T3a	10 (40)
T3b/T4	3 (12)
Pathological N stage, n (%)	
N0	22 (88)
N1	3 (12)
ISUP grade group at final pathology, n (%)	
1	0 (0)
2	5 (20)
3	12 (48)
4	4 (16)
5	4 (16)
Positive surgical margins, n (%)	
R0	15 (60)
R1	10 (40)
SNs identified at pathology, n (median, IQR)	92 (4, 2–5)
Overall LNs identified at pathology, n (median, IQR)	527 (22, 12–27)
Positive SNs, n (patient, %)	5 (3, 12)
Overall positive LNs, n (patient, %)	9 (3, 12)
Follow-up (mo), median (IQR)	18 (15–20)
BMI = body mass index; IQR = interquartile range; ISUP = International Society of Urological Pathology; LN = lymph node; PSA = prostate-specific antigen; SN = sentinel node.	

3.3. Pathology, follow-up, and postoperative complications

At final histopathology, nine tumour-positive nodes were identified (three patients, 12% [3/25]; [Table 1](#)). Of these, five were SNs and four were non-SNs. All patients with positive nodes had at least one positive SN ([Table 1](#)), which is in line with earlier reports on similar procedures [22]. This also means that no false-negative SNs occurred. Of the SNs, three were removed under the guidance of the DROP-IN gamma probe and Firefly fluorescence camera (where one of these was located outside the ePLND template), and two were removed as part of the ePLND template.

Overall, the median follow-up was 18 mo (IQR: 15–20). Five patients (20%) had BCR. All these patients had a positive SN and/or positive resection margin (see Supplementary Table 1). All these five patients received follow-up PSMA-PET, but only one patient showed the signs of pelvic lymphatic metastasis.

Table 2 – In vivo and ex vivo sentinel node detection according to the DROP-IN gamma probe versus the traditional laparoscopic gamma probe versus fluorescence laparoscope

General information						
No. of patients	Injected tracer	Median injected radioactive dose (MBq)		Median time between radioactive injection and surgery (h)		
25	48% ICG- ^{99m} Tc-nanocolloid 52% ^{99m} Tc-nanocolloid + ICG	205.6		5.4		
In vivo guidance						
	DROP-IN gamma probe (n=25)	Laparoscopic gamma probe (n=14)		Fluorescence (n=25)		
SNs pursued, n	47	21		46		
SNs identified, n (%)	47 (100)	16 (76.2)		42 (91.3)		
Signal quantification, median (IQR [counts/s])	844 (530–1550)	438 (205–825)		NA		
% of SNs divided over anatomical locations	Identified	Not identified (%)	Identified	Not identified	Identified	Not identified
Obturator L, n (%)	14 (30)	0	5 (24)	0 (0)	12 (26)	1 (2)
External L, n (%)	8 (17)	0	2 (10)	1 (5)	8 (17)	0 (0)
Internal L, n (%)	2 (4)	0	0 (0)	0 (0)	2 (4)	0 (0)
Common L, n (%)	2 (4)	0	1 (5)	0 (0)	2 (4)	0 (0)
Paravesical L, n (%)	1 (2)	0	0 (0)	0 (0)	1 (2)	0 (0)
Obturator R, n (%)	11 (23)	0	5 (24)	2 (10)	10 (22)	1 (2)
External R, n (%)	5 (11)	0	2 (10)	1 (5)	4 (9)	1 (2)
Internal R, n (%)	1 (2)	0	0 (0)	0 (0)	0 (0)	1 (2)
Common R, n (%)	2 (4)	0	1 (5)	1 (5)	2 (4)	0 (0)
Paravesical R, n (%)	1 (2)	0	0 (0)	0 (0)	1 (2)	0 (0)
Ex vivo confirmation						
	DROP-IN gamma probe (n=25)	Laparoscopic gamma probe (n=25)		Fluorescence (n=25)		
SNs pursued, n	47	47		46		
SNs identified, n (%)	47 (100)	47 (100)		44 (96)		
Signal quantification, median (IQR [counts/s])	1255 (609–2222)	368 (226–937)		NA		

ICG = indocyanine green; L = left; NA = not available; R = right; SN = sentinel node.

Postoperative complications are reported in Supplementary Table 2. None of these complications were related to the use of the DROP-IN gamma probe.

4. Discussion

With the rapid expansion of robotic surgery, an increased demand has been observed for image-guided technologies [10]. This has resulted not only in the integration of Firefly fluorescence within the da Vinci robot [10,15] and the availability of DROP-IN ultrasound [23], but now also in the availability of a robotic-tailored radioguidance modality (ie, the DROP-IN gamma probe). By evaluating the technical implementation and safety profile of the DROP-IN gamma probe concept during SN detection, we were able to quantify the impact that the technology provides relative to the use of traditional laparoscopic gamma probes and fluorescence guidance. In detail, the following aspects were identified.

First, no adverse events related to the use of the DROP-IN probe were observed, suggesting the safety of this novel technology.

Second, the increased in vivo detection rate of the DROP-IN gamma probe compared with the laparoscopic probe (ie, 100% vs 76%) can be attributed to improved manoeuvrability and autonomous probe control by the operating

surgeon. The anatomical restrictions, encountered with the laparoscopic probe, could theoretically be overcome by using additional trocars that provide more points of entry into the abdomen. However, there is no way the surgeon can obtain easy robotic access for positioning of this probe, while this can readily be achieved with the DROP-IN. The improved nodal identification with the DROP-IN means that future studies can investigate whether it becomes possible to resect SNs in the presacral and pararectal regions (10%) [5], without the risk of surgical complications.

Third, we demonstrated that the DROP-IN technology could well lead to superior in vivo detection sensitivity compared to fluorescence imaging (100% vs 91.3% detected SNs). Improved fluorescence detection following exposure of the excised tissues (ie, ex vivo) indicated that signal attenuation was the limiting factor in vivo, as reported previously [17,18]. The impact of tissue attenuation may be related to the high BMI of our patients [24]. Nevertheless, symbiotic use of the DROP-IN gamma probe was considered valuable for nodal identification [10]: fluorescence imaging provides real-time high-resolution images and optical confirmation of SN localisation [25].

Limitations of our study are represented by its small sample size and the fact that approximately 50% of the SNs were already removed during standard ePLND or left in situ due to high-risk anatomical locations. In addition, the

laparoscopic gamma probe was omitted in some locations that could not be reached. Both decisions were taken based on the surgeon's discretion, prioritising patient care over the study. Clearly, future multicentre studies in larger patient groups are required to define the oncological benefit of the individual guidance modalities.

All findings combined underscore the intraoperative detection accuracy benefits from having the operating surgeon autonomously controlling a DROP-IN probe and being able to benefit from the full rotational freedom of the robotic surgical instruments. This engineering effort strengthens the future for robotic radioguidance procedures. As the probe detection is defined by the ^{99m}Tc isotope, its use can be extended to other tracers harbouring the same isotope, for example, ^{99m}Tc -PSMA-I&S. In fact, we have already been able to transfer PSMA-targeted salvage surgery, initially pursued in an open setting by Maurer et al [26] and Horn et al [27], to the robotic setting [28]. Knowing that the SN- and PSMA-targeted image-guidance techniques highlight complementary features [29], the first technique targeting micrometastases and the latter >2 mm macrometastases [10], both approaches could coexist in the primary setting.

5. Conclusions

The current study has helped deepen the insight into the value that the DROP-IN technology provides in comparison with the traditional laparoscopic gamma probe and the Firefly fluorescence camera. The superior performance found indicates that the DROP-IN technology provides a valuable tool for robotic surgeries that are realised under the guidance of nuclear medicine.

Author contributions: Matthias N. van Oosterom had full access to all the data in the study and takes responsibility for the integrity of the data and the accuracy of the data analysis.

Study concept and design: van Oosterom, F.W.B. van Leeuwen, van der Poel.

Acquisition of data: Meershoek, van Oosterom, Wit, P.J. van Leeuwen, van der Poel.

Analysis and interpretation of data: Dell'Oglio, Maurer, P.J. van Leeuwen, van der Poel, F.W.B. van Leeuwen, van Oosterom.

Drafting of the manuscript: Dell'Oglio, F.W.B. van Leeuwen, van Oosterom.
Critical revision of the manuscript for important intellectual content: Dell'Oglio, Maurer, P.J. van Leeuwen, van der Poel, F.W.B. van Leeuwen, van Oosterom.

Statistical analysis: Dell'Oglio, van Oosterom.

Obtaining funding: F.W.B. van Leeuwen, van der Poel.

Administrative, technical, or material support: Meershoek, Wit, Dell'Oglio, van Oosterom.

Supervision: F.W.B. van Leeuwen, van der Poel, van Oosterom.

Other: None.

Financial disclosures: Matthias N. van Oosterom certifies that all conflicts of interest, including specific financial interests and relationships and affiliations relevant to the subject matter or materials discussed in the manuscript (eg, employment/affiliation, grants or funding, consultancies, honoraria, stock ownership or options, expert

testimony, royalties, or patents filed, received, or pending), are the following: None.

Funding/Support and role of the sponsor: This research was supported by an NWO-TTW-VICI grant (TTW 16141) and a non-limiting Intuitive research grant. The clinical trial was supported with hardware by Eurorad S.A. and Hamamatsu Photonics K.K.

Acknowledgements: The authors would like to gratefully acknowledge the surgical staff of the NKI-AVL (Amsterdam, the Netherlands) for assistance in the operating room. In addition, the authors would like to thank Florian van Beurden (LUMC, Leiden, the Netherlands) for his assistance with the phantom evaluation (as shown in the Supplementary material). Furthermore, they would like to thank Nikolas Duszenko (LUMC, Leiden, the Netherlands) for providing the voice-over narration as used in our movie.

Appendix A. Supplementary data

The Surgery in Motion video accompanying this article can be found in the online version at doi:<https://doi.org/10.1016/j.eururo.2020.10.031> and via www.europeanurology.com.

References

- [1] Seiler R, Studer UE, Tschan K, Bader P, Burkhard FC. Removal of limited nodal disease in patients undergoing radical prostatectomy: long-term results confirm a chance for cure. *J Urol* 2014;191:1280–5.
- [2] Touijer KA, Mazzola CR, Sjoberg DD, Scardino PT, Eastham JA. Long-term outcomes of patients with lymph node metastasis treated with radical prostatectomy without adjuvant androgen-deprivation therapy. *Eur Urol* 2014;65:20–5.
- [3] Abdollah F, Karnes RJ, Suardi N, et al. Impact of adjuvant radiotherapy on survival of patients with node-positive prostate cancer. *J Clin Oncol* 2014;32:3939–47.
- [4] European Association of Urology. Guidelines on prostate cancer. 2019.
- [5] Joniau S, Van den Bergh L, Lerut E, et al. Mapping of pelvic lymph node metastases in prostate cancer. *Eur Urol* 2013;63:450–8.
- [6] Mattei A, Fuechsel FG, Bhatta Dhar N, et al. The template of the primary lymphatic landing sites of the prostate should be revisited: results of a multimodality mapping study. *Eur Urol* 2008;53:118–25.
- [7] Wawroschek F, Wagner T, Hamm M, et al. The influence of serial sections, immunohistochemistry, and extension of pelvic lymph node dissection on the lymph node status in clinically localized prostate cancer. *Eur Urol* 2003;43:132–6, discussion 137.
- [8] Meinhardt W, van der Poel HG, Valdes Olmos RA, Bex A, Brouwer OR, Horenblas S. Laparoscopic sentinel lymph node biopsy for prostate cancer: the relevance of locations outside the extended dissection area. *Prostate Cancer* 2012;2012:751753.
- [9] Hruby S, Englberger C, Lusuardi L, et al. Fluorescence guided targeted pelvic lymph node dissection for intermediate and high risk prostate cancer. *J Urol* 2015;194:357–63.
- [10] van Leeuwen FWB, Winter A, van Der Poel HG, et al. Technologies for image-guided surgery for managing lymphatic metastases in prostate cancer. *Nat Rev Urol* 2019;16:159–71.
- [11] Wit EMK, Acar C, Grivas N, et al. Sentinel node procedure in prostate cancer: a systematic review to assess diagnostic accuracy. *Eur Urol* 2017;71:596–605.
- [12] Wawroschek F, Vogt H, Weckermann D, Wagner T, Harzmann R. The sentinel lymph node concept in prostate cancer - first results of

- gamma probe-guided sentinel lymph node identification. *Eur Urol* 1999;36:595–600.
- [13] van Oosterom MN, Simon H, Mengus L, et al. Revolutionizing (robot-assisted) laparoscopic gamma tracing using a drop-in gamma probe technology. *Am J Nucl Med Mol Imaging* 2016;6:1–17.
- [14] Meershoek P, van Oosterom MN, Simon H, et al. Robot-assisted laparoscopic surgery using DROP-IN radioguidance: first-in-human translation. *Eur J Nucl Med Mol Imaging* 2019;46:49–53.
- [15] KleinJan GH, van den Berg NS, de Jong J, et al. Multimodal hybrid imaging agents for sentinel node mapping as a means to (re) connect nuclear medicine to advances made in robot-assisted surgery. *Eur J Nucl Med Mol Imaging* 2016;43:1278–87.
- [16] Pandey A, Dell'Oglio P, Mazzone E, Mottrie A, Geert De N. Usefulness of the indocyanine green (ICG) immunofluorescence in laparoscopic and robotic partial nephrectomy. *Arch Esp Urol* 2019;72:723–8.
- [17] Meershoek P, Buckle T, van Oosterom MN, KleinJan GH, van der Poel HG, van Leeuwen F. Can fluorescence-guided surgery help identify all lesions in unknown locations or is the integrated use of a roadmap created by preoperative imaging mandatory? A blinded study in prostate cancer patients. *J Nucl Med* 2020;61:834–41.
- [18] Jeschke S, Lusuardi L, Myatt A, Hruba S, Pirich C, Janetschek G. Visualisation of the lymph node pathway in real time by laparoscopic radioisotope- and fluorescence-guided sentinel lymph node dissection in prostate cancer staging. *Urology* 2012;80:1080–6.
- [19] Briganti A, Larcher A, Abdollah F, et al. Updated nomogram predicting lymph node invasion in patients with prostate cancer undergoing extended pelvic lymph node dissection: the essential importance of percentage of positive cores. *Eur Urol* 2012;61:480–7.
- [20] Fossati N, P-PM Willemsse, Van den Broeck T, et al. The benefits and harms of different extents of lymph node dissection during radical prostatectomy for prostate cancer: a systematic review. *Eur Urol* 2017;72:84–109.
- [21] Assel M, Sjöberg D, Elders A, et al. Guidelines for reporting of statistics for clinical research in urology. *Eur Urol* 2019;75:358–67.
- [22] KleinJan GH, van den Berg NS, Brouwer OR, et al. Optimisation of fluorescence guidance during robot-assisted laparoscopic sentinel node biopsy for prostate cancer. *Eur Urol* 2014;66:991–8.
- [23] Hughes-Hallett A, Pratt P, Mayer E, et al. Intraoperative ultrasound overlay in robot-assisted partial nephrectomy: first clinical experience. *Eur Urol* 2014;3:671–2.
- [24] KleinJan GH, van Werkhoven E, van den Berg NS, et al. The best of both worlds: a hybrid approach for optimal pre- and intraoperative identification of sentinel lymph nodes. *Eur J Nucl Med Mol Imaging* 2018;45:1915–25.
- [25] Harke NN, Godes M, Wagner C, et al. Fluorescence-supported lymphography and extended pelvic lymph node dissection in robot-assisted radical prostatectomy: a prospective, randomized trial. *World J Urol* 2018;36:1817–23.
- [26] Maurer T, Robu S, Schottelius M, et al. (99m)Technetium-based prostate-specific membrane antigen-radioguided surgery in recurrent prostate cancer. *Eur Urol* 2019;75:659–66.
- [27] Horn T, Kronke M, Rauscher I, et al. Single lesion on prostate-specific membrane antigen-ligand positron emission tomography and low prostate-specific antigen are prognostic factors for a favorable biochemical response to prostate-specific membrane antigen-targeted radioguided surgery in recurrent prostate cancer. *Eur Urol* 2019;76:517–23.
- [28] van Leeuwen FWB, van Oosterom MN, Meershoek P, et al. Minimal-invasive robot-assisted image-guided resection of prostate-specific membrane antigen-positive lymph nodes in recurrent prostate cancer. *Clin Nucl Med* 2019;44:580–1.
- [29] Hinsenveld FJ, Wit EMK, van Leeuwen PJ, et al. Prostate-specific membrane antigen PET/CT combined with sentinel node biopsy for primary lymph node staging in prostate cancer. *J Nucl Med* 2020;61:540–5.